International Journal of Heat and Technology
Vol. 36, No. 3, September, 2018, pp. 913-918
Journal homepage: http://iieta.org/Journals/IJHT

Flow characteristics of the new type of mixer in wastewater treatment

Fei Tian[1,3,*], Weidong Cao[2], Xiaoli Dai[1], Mingxiong Ou[2]

[1] School of energy and power engineering, Jiangsu University, Zhenjiang 212013, China
[2] National Research Center of Pumps and Pumping System Engineering and Technology, Zhenjiang 212013, China
[3] Yatai Pump &Valve Co., Ltd., Taizhou, Jiangsu 220000, China

Corresponding Author Email: tianfei@ujs.edu.cn

https://doi.org/10.18280/ijht.360318

Received: 9 February 2018
Accepted: 18 June 2018

Keywords:
new type of mixer, CFD, flow filed, simulation, fluid dynamics

ABSTRACT

This paper studies the flow field of a new type of submersible mixer with two impellers and six blades in the wastewater treatment pool by using large-scale software, such as Pro/engineering, FLUENT 15.0 and ICEM. After that, it numerically simulates the wastewater treatment pool using the RNG k-ε turbulent model and the mobile coordinate measuring system, and analyzes the macro fluid field and flow field distribution of the sections. The fluid in the wastewater treatment pool can be propelled by the new type of mixer, and the fluid flows along the axial direction of the submersible mixer and diffuses radially. Eight water and sludge cycles are formed in the pool, and the fluid in the pool forms two high-flow region and eight low-flow regions. The velocity distribution in the pool is distributed symmetrically along the plane Z=0m and the plane X=1.75m. As the new type of mixer is installed close to the bottom of the pool, the position with the maximum velocity offsets gradually to the bottom of the pool with the increasing distance to the impeller. The new type of mixer is different from the traditional submersible mixer, in that the fluid mixed by the new one can circulate fully on both sides of the submersible mixer. Consequently, this new type of submersible mixer can mix more fluid, and there will be a smaller dead zone in the whole pool with less sludge at the bottom. This simulation method can guide the application of mixers in the practical wastewater treatment.

1. INTRODUCTION

It has been almost 60 years since the mixer was invented. Now, as the essential equipment for wastewater treatment, it is applied widely in agriculture, petroleum, manufacturing and chemical industry, etc. The utilization rate of mixers is up to 50% in the wastewater treatment equipment. This kind of mixer is also called the submersible mixer because it is installed under water. The fluid stirred by the submersible mixer in the pool is complex and affected by the walls of the pool and the mixer. In the recent 20 years, many researchers have studied the submersible mixer and obtained many meaningful results.

Currently, a mixer impeller has two or three blades. In this paper, the new type of submersible mixer has two impellers and six blades, and summarizes its flow field characteristics.

2. STUDY OBJECT

The wastewater treatment pool is 10m long, 3.5m wide and 5.5m deep. As shown in Figure 1, the new type of mixer is a submersible mixer, which has two impellers with six blades. The motor is in the middle, and on each side is an impeller with three blades. The diameter of the impeller is 380mm, the hub diameter 90mm, and the rotational speed 680rnp. Both impellers rotate clockwise. As shown in Figure 2, the new type of mixer is installed 1m above the bottom in the middle of the pool. The coordinate O' of the centre position of the mixer is (1.75, 1, 0). The fluid model is built by the software PRO/E, and the inlets and outlets of the impellers are shown in Figure 1.

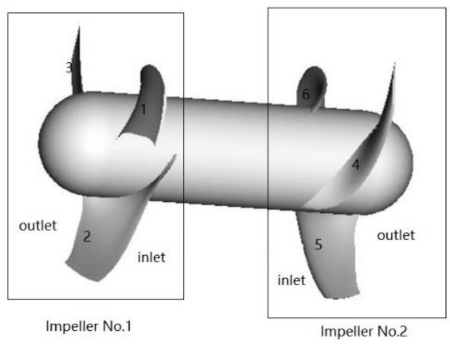

Figure 1. New type of submersible mixer

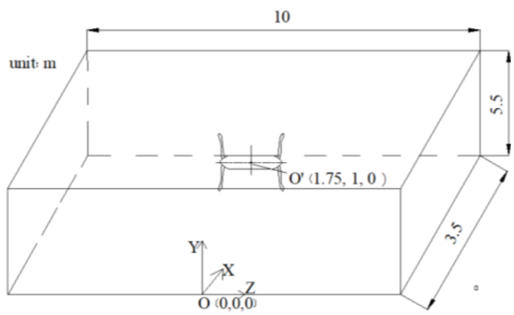

Figure 2. Size of pool and the location of submersible mixer

Table 1. Parameters of the submersible mixer

D (mm)	n (rnp)	P (KW)	F (N)	Z
368	680	1.5	3.5	6

In order to simplify the calculation, the mixing medium of the mixer is water, whose density is 1×10^3kg/m^3 and viscosity is 1×10^3kg/m·s at 20℃ and atmospheric pressure.

3. SIMULATION

3.1 Grid

The large-scale software ICEM is used to divide the grid, and meshes near the interfaces between the impellers and the pool are local mesh refined [6-12]. There are a total of about 3,000,000 grid nodes, with 600,000 nodes of water in each impeller and 1,700,000 nodes of water in the pool, as shown in Figure 3-Figure 5.

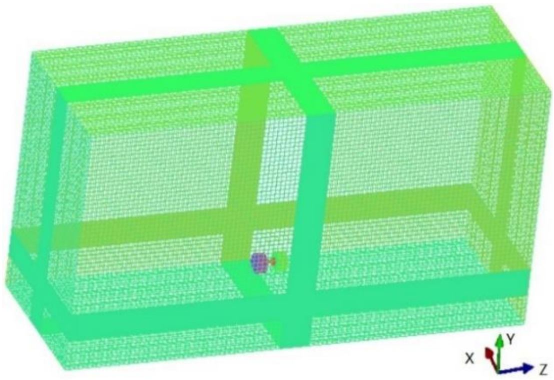

Figure 3. Grid of the pool

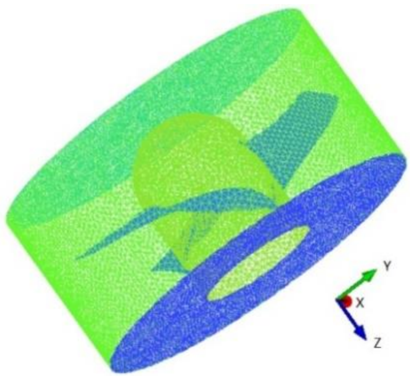

Figure 4. Grid of impeller 1

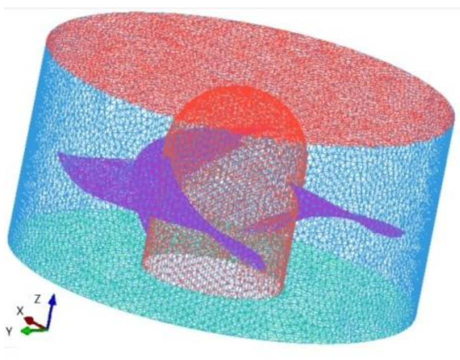

Figure 5. Grid of impeller 2

3.2 Calculation equation

For the fluid, that cannot be compressed, its CFD expressions include the continuity equation, the momentum equation and the RNG *k-ε* turbulence equation.

$$\frac{\partial u_j}{\partial x_j}=0$$

$$\rho\frac{\partial u_i}{\partial t}+u_j\rho\frac{\partial u_i}{\partial x_j}=-\frac{\partial p}{\partial x_i}+\mu\frac{\partial^2 u_i}{\partial x_j^2}+\rho f_i$$

$$\frac{\partial(\rho k)}{\partial t}+\frac{\partial(\rho k u_i)}{\partial x_i}=\frac{\partial}{\partial x_i}[\alpha_k\mu\frac{\partial k}{\partial x_j}]+G_k+\rho\varepsilon$$

$$\frac{\partial(\rho\varepsilon)}{\partial t}+\frac{\partial(\rho\varepsilon u_i)}{\partial x_i}=\frac{\partial}{\partial x_i}[\alpha_\varepsilon\mu\frac{\partial\varepsilon}{\partial x_j}]+\frac{C_{1\varepsilon}}{k}G_k-C_{2\varepsilon}\rho\frac{\varepsilon^2}{k}$$

In the expressions, i, j=1,2,3; $\rho\frac{\partial u_i}{\partial t}$ is non-constant, $u_j\frac{\partial u_i}{\partial x_j}$ is convection, $\mu\frac{\partial^2 u_i}{\partial x_j^2}$ is diffusion, ρf_i is volume force, $C_{1\varepsilon}$=1.42, and $C_{2\varepsilon}$=1.68, k is the turbulence power, and ε is the dissipation rate [1-12].

3.3 Fluent boundary conditions and parameters

The study adopts the fluid mechanics software FLUENT15.0, the finite volume discretization method as well as the SIMPLE method and the RNG *k-ε* turbulence model. It is assumed that the surfaces of all walls, the stirring axis and the blades are in the non-slip condition; and the stirring blades and stirring axis are set at the appropriate rotation velocities. The convergence criterion is that the residual absolute values of all variables are less than 10^{-5} [8-25].

4. SIMULATION ANALYSIS

The plane X=1.75m, plane Z=0m and plane Y=1m are parallel to the long sidewall, the short sidewall and the bottom of the pool, respectively. The axis of the mixer is in plane X=1.75m, and plane Y=1m. Figure 6 is the streamlines in plane X=1.75m, plane Y=1m, plane Z=0m and the whole pool. The fluid in the pool is divided into ten areas by those three planes. The average velocity of the fluid in the pool can be obtained, which is about 0.12m/s, greater than 0.1m/s. It meets the standard for submersible operation. Because of the high-speed rotation of the impellers, the fluid nearby absorbed into the impellers obtain great kinetic energy. The high-speed fluid rushes out from the impellers, and suck the nearby fluid. They flow together, forming two high-speed areas in the axis direction of the mixer. The fluid in the pool can be propelled by the new type of submersible mixer. It flows along the axial direction of the submersible mixer and diffuses radially. The high-speed fluid changes its flow direction to the long sidewall, the bottom and the top of the pool when it meets the short sidewall. At the same time, the fluid near the mixer, which is at the bottom and center of the pool, is sucked into the impellers. So four water cycles are formed above the high-speed fluid area, and other four ones below the high-speed fluid area. However, the fluid velocities in the eight areas are lower than those in the other two high-speed ones.

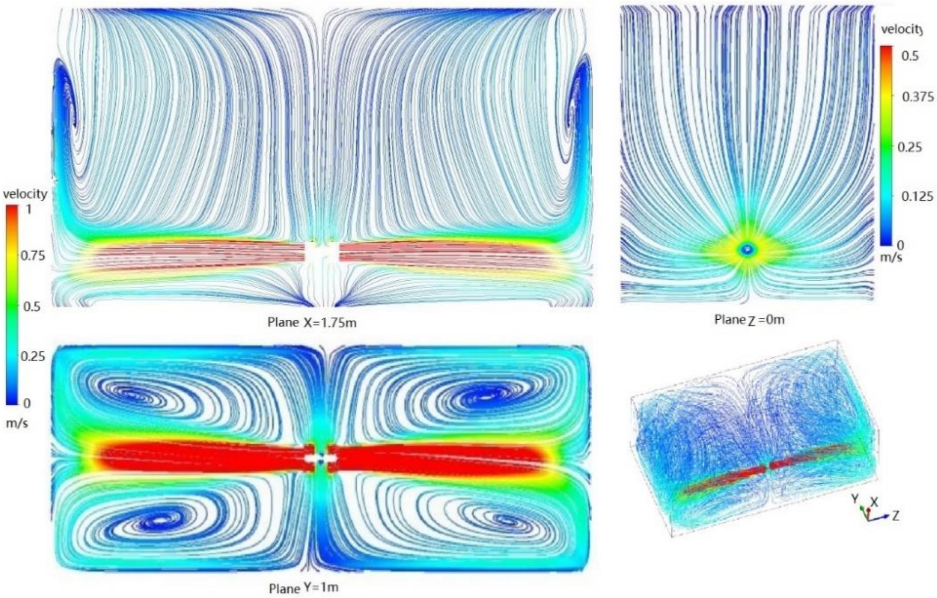

Figure 6. Streamline

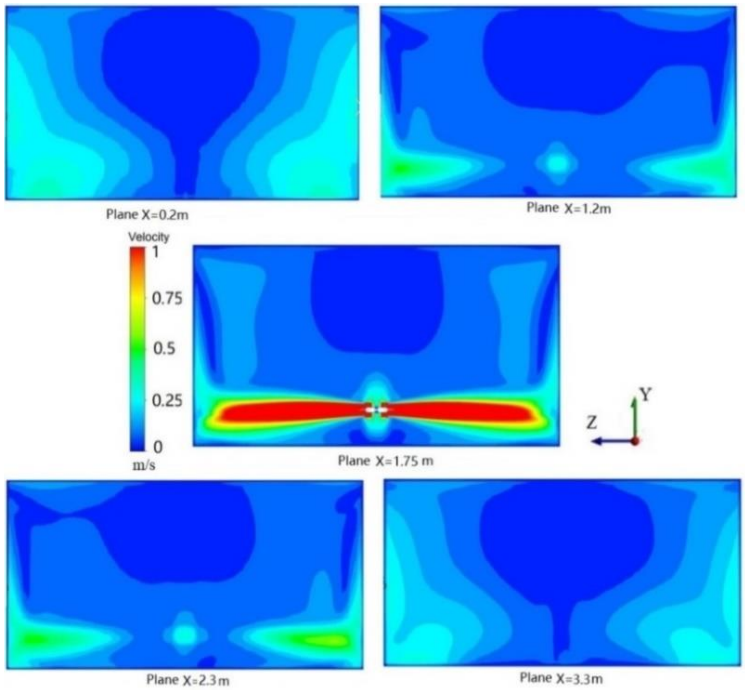

Figure 7. Velocity distribution of section X

The velocity distributions of section X, section Y and section Z are respectively shown in Figure 7, 8 and 9. As can be clearly seen, the fluid flow is symmetrically distributed from the centre of the mixer. In Figure 7, plane X=1.2m and plane X=2.3m, which are at the same distance to plane X=1.75, have the same velocity distribution. Plane X=0.2m and plane X=3.3m, which are at the same distance to plane X=1.75, have the same velocity distribution. In Figure 8, the sections are distributed symmetrically from plane Z=0m, and the velocity distributions of these sections are symmetrical along the axis of the mixer. As the height increases along the axis of the mixer, from plane Y=1m to plane Y=5m, the fluid velocity decreases gradually. In Figure 9, the velocity of the fluid near the impellers is much greater than that of the fluid near the pool level. As shown in Figure 7-9, the velocity of the fluid in the center of the pool and above the mixer is lower than 0.1m/s. Under gravity, the sludge will sink to the bottom of the pool. Due to the two high-speed fluid areas, the sludge will be drawn into the high-velocity fluid and flow with it during the sinking process. So the sludge will not sink and stay at the bottom of the pool.

Since the velocity in plane X=1.75m is distributed symmetrically along the Y-axis, the curve of velocity in the right half of plane X=1.75m is obtained from the software FLUENT 15.0. The velocity distribution curves of line Z=0.4m, line Z=1m, line Z=3m and line Z=4m in plane X=1.75m are shown in Figure 10. The curves of lines Z=0.4m and Z=1m are both of a saddle shape, with a lower velocity in Y=1m under the effect of the impeller hub. The closer it is to the hub, the greater impact there will be on the velocity of the fluid at the center position of Y=1m, and the lower its velocity will be near Y=1m. Two maximum velocity peaks occur in Y=0.92m and Y=1.08m, and the velocity in Y=0.92m is slightly larger than that in Y=1.08m. The maximum velocity of line Z=3m and line Z=4m is in Y=0.9m and Y=0.85m, respectively. The position with the maximum velocity will offset to the bottom of the pool with the increasing distance to the impellers. As the submersible mixer is installed close to the bottom of the pool, the fluid flow shifts toward the bottom of the pool gradually, where the attachment phenomenon occurs.

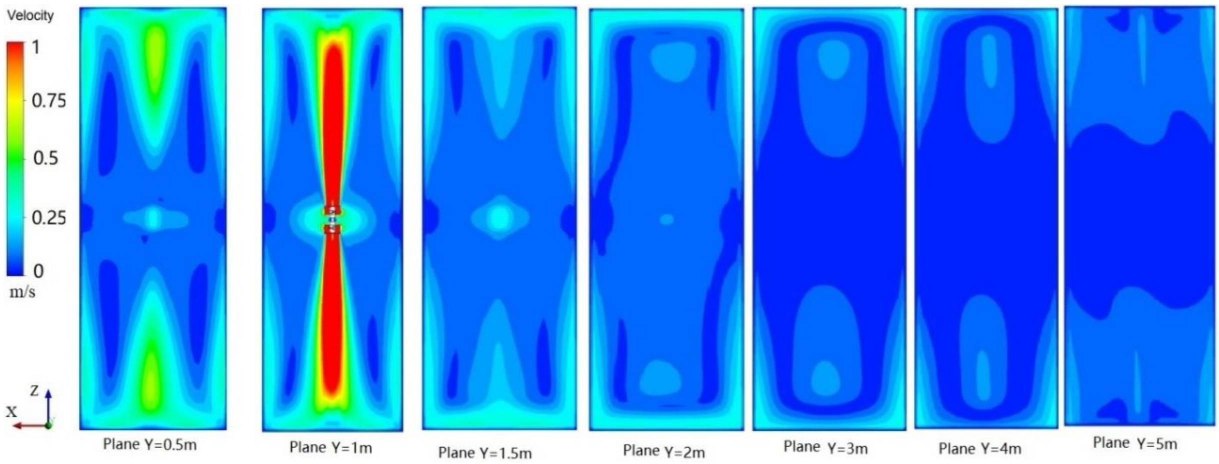

Figure 8. Velocity distribution of section Y

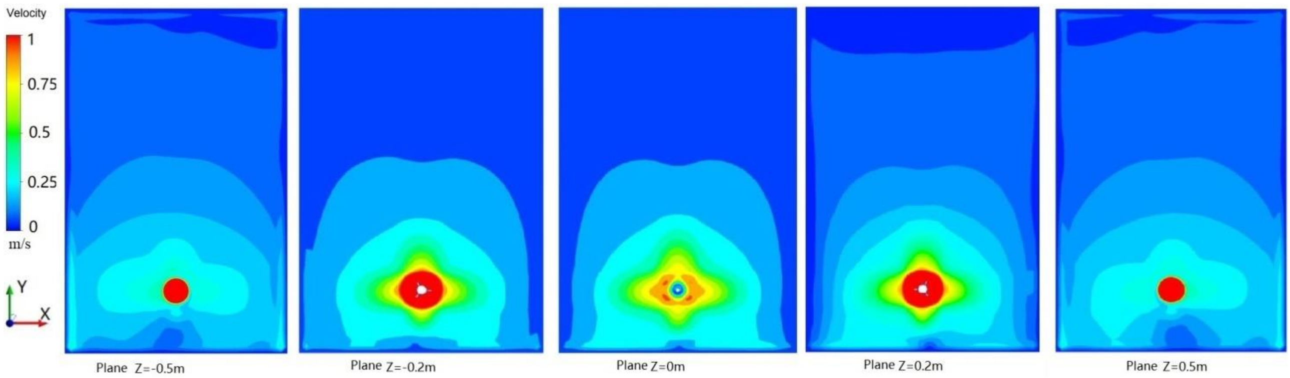

Figure 9. Velocity distribution of section Z

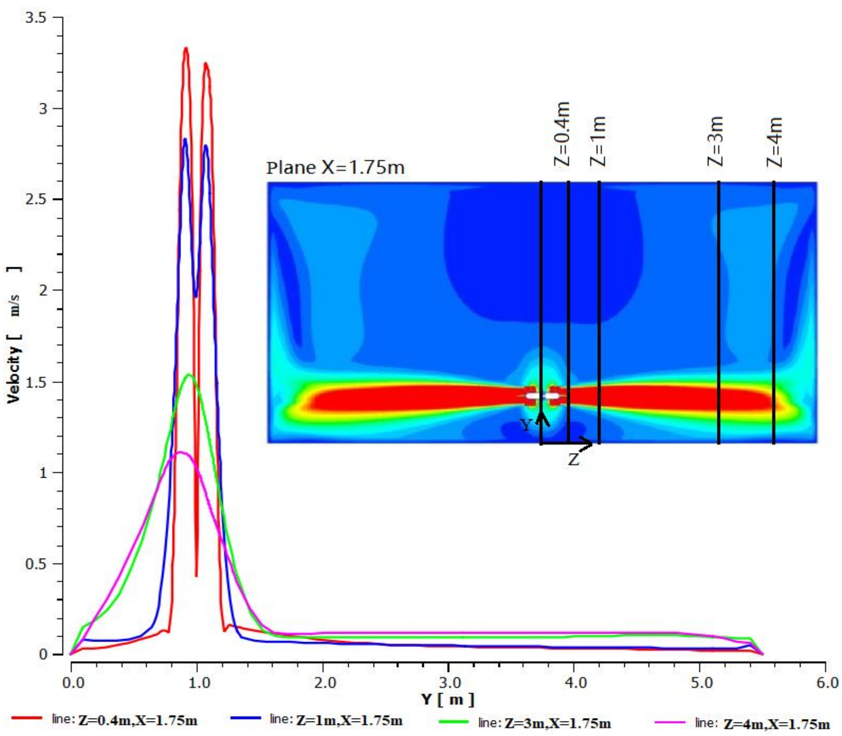

Figure 10. Velocity distribution of Line Z (Plane X=1.75m)

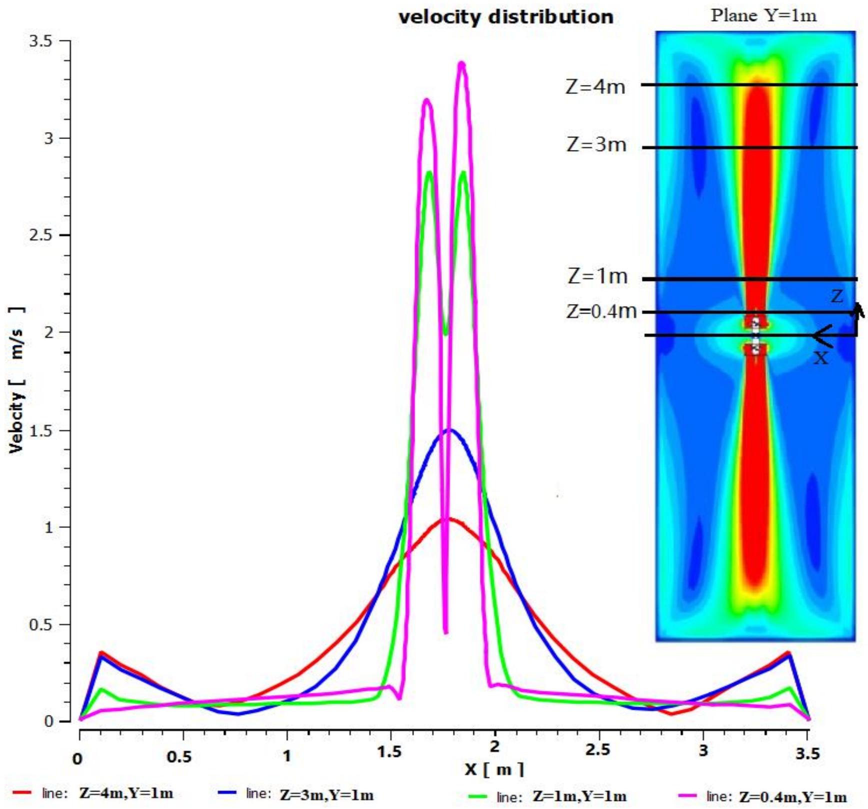

Figure 11. Velocity distribution of Line Z (Plane Y=1m)

The velocity distribution curves of line Z=0.4m, line Z=1m, line Z=3m and line Z=4m in plane Y=1m are shown in Figure 11. The curves of line Z=0.4m and Z=1m are both of a saddle shape, with a lower velocity in X=1.75m under the effect of the impeller hub. Two maximum velocity peaks occur in X=1.6m and X=1.9m, and the velocity in X=1.9m is slightly larger than that in X=1.6m. The maximum velocity of line Z=3m and line Z=4m is both in Y=1.75m because the mixer is installed to the sidewall of the pool symmetrically.

5. RESULTS

According to the working condition of the new type of mixer, the fluid in the wastewater treatment pool is simulated using FLUENT15.0. The results show:

(1) The fluid in the wastewater treatment pool can be propelled by the new type of mixer. The fluid flows along the axial direction of the mixer and diffuses radially. Eight water cycles with sludge are formed in the pool, and the fluid in the pool forms two high-flow regions and eight low-flow regions.

(2) The velocity distribution in the pool is symmetrical along the plane Z=0m and the plane X=1.75m. As the new type of mixer is installed close to the bottom of the pool, the position with the maximum velocity shifts gradually to the bottom of the pool with the increasing distance to the impeller.

(3) The traditional mixer with one impeller can only stir and propel the fluid in front of the outlet of the impeller in the new type of mixer. But the fluid in the pool mixed by the new type of mixer can form full circulation on both sides of the mixer.

ACKNOWLEDGEMENTS

This work was supported by Natural Science Foundation of Jiangsu Province (Grant Nos.: BK20160521, NO.: BK20170554), Jiangsu Postdoctoral Funding Program (2018K017A) Key Development Project of Zhenjiang City (Grant Nos.: SH2017049), the National Natural Science Foundation of China (Grant Nos.: 31601676)

REFERENCE

[1] Beltaos S, Rajaratnam N. (1973). Plane turbulent impinging jets. Journal of Hydraulic Research 11(1): 29-59. https://doi.org/10.1080/00221687309499789

[2] Bradbury LJS. (1972). The impact of an axisymmetric jet onto a normal ground. Aeroautical Quarterly 23: 141-147. https://doi.org/10.1017/S0001925900006016

[3] Lan ZY. (1997). Impinging jet. Beijing: Ocean press.

[4] Tian F, Shi WD, Chen B, Cao WD. (2010). Study on installation position of sewage treatment mixer. ASME FEDSM2010 1: 329-334. https://doi.org/10.1115/FEDSM-ICNMM2010-30988

[5] Dong ZY. (2005). Jet mechanics. Beijing: Science Press.

[6] Tian F, Shi WD, Cao WD, Zhang DS, Li W. (2008). Inner flow of new type streamline shape XCK mixer with two blades. Drainage and Irrigation Machinery 26(6): 6-9.

[7] Shi WD, Zhang L, Chen B, Jiang T, Zhang H. (2012). Influence of gap on pressure pulsation and radial force of centrifugal pumps. Journal of Drainage and Irrigation Machinery Engineering 30(5): 260-264.

[8] Guo B., Liu HL, Tan MG. (2016). Effect of circumferential setting position of diffuser in concentric volute on impeller radial thrust in centrifugal pump. Journal of Drainage and Irrigation Machinery Engineering 34(3): 204-209.

[9] Lee SL. (1965). Axisymmetrical turbulent swirling jet.

Journal of Applied Mechanics 32(2): 258-262. https://doi.org/10.1115/1.3625793
[10] Wang W, Shi WD, Jiang XP. (2016). Optimization design of multistage centrifugal pump impeller by orthogonal experiment and CFD. Journal of Drainage and Irrigation Machinery Engineering 34(3): 191-197.
[11] Loitsyanskii LG. (1953). The propagation of a twisted jet in an unbounded space filled with the same fluid. I Prikladnaya Matetnatiza Mekhanika 17: 3-16.
[12] Tian F, Shi WD, Chen B. (2011). Flow Analysis and Measurement of Wastewater Treatment Mixer with Dome. China Academic Journal Electronic Publishing House 42(3): 96-99.
[13] Bosco F, Mollea C, Marmo L. (2018). Application of scenedesmus obliquus in the treatment of a real wastewater. Chemical Engineering Transactions 64: 475-480. https://doi.org/10.3303/CET1864080
[14] Sawasdee V, Pisutpaisal N. (2018). Microbial community from tannery wastewater in microbial fuel cell. Chemical Engineering Transactions 64: 397-402. https://doi.org/10.3303/CET1864067
[15] Donaldson C, Snedeker RS. (1971). A study of free jet impingement. Part 1: Mean properties of free and impinginq jets. J. Fluid Mech 15: 337-367.
[16] Tian F, Shi WD, Lu X, Chen B, Ou M. (2012). Numerical simulation of the submersible mixer with three blades. Journal of Drainage and Irrigation Machinery Engineering 30(1): 11-14.
[17] Tian F, Shi WD, Cao W, Chen B, Zhang D. (2009). Numerical simulation of mixer power consumptions in different ponds. Journal of Drainage and Irrigation Machinery Engineering 27(3): 140-143.
[18] Li WQ, Li W, Shi WD. (2016). A review of engine cooling water pump. Journal of Drainage and Irrigation Machinery Engineering 34(1): 9-17.
[19] Tian F, Shi WD, Jiang H. (2014). Matching criterion of submersible mixer and pool. Advances in Mechanical Engineering (4): 1-5. https://doi.org/10.1155/2014940904
[20] Cheng QG, Wu SF, Wu YL, Liu SH, Zhang YC. (2006) Numerical prediction of cavitating flow in a Kaplan turbine. Journal of Engineering Thermophysics 27(5): 769-771.
[21] Tian F, Shi WD, Jiang H, Zhang QH, (2014). A study on two-phase flow of multiple submersible mixers based on rigid-lid assumption. Advances in Mechanical Engineering (5): 1-6. https://doi.org/10.1155/2014/531234
[22] Xu YH, Zhang QH, Shi WD. (2016). Design of new type diffuser of plastic well pump and pulsation characteristics of internal pressure. Journal of Drainage and Irrigation Machinery Engineering 34(1): 18-25.
[23] Ross DG. (1978). On integral method solutions for modeling swirling jets and plumes. Appl. Sci. Res. 34(2-3): 273-298.
[24] Steiger MH, Bloom MH. (1962). Axially symmetric laminar free mixing with large swirl. Journal of Heat Transfer. Trans, ASME, Series C 83: 370-374. https://doi.org/10.1115/1.3684400
[25] Wang DX, Cao WD, Zhang YN. (2016). Effects of volute cross-section shape and impeller position on volute type axial flow pump performance. Journal of Drainage and Irrigation Machinery Engineering 34(2): 105-109.